A highly selective cell-based fluorescent biosensor for genistein detection

Engineering Microbiology 3 (2023) 100078

Contents lists available at ScienceDirect

Engineering Microbiology

journal homepage: www.elsevier.com/locate/engmic

Original Research Article

A highly selective cell-based fluorescent biosensor for genistein detection

Lucy Fang-I Chao[#], Dany Liu[#], Verena Siewers[*]

Department of Life Sciences, Division of Systems and Synthetic Biology, Chalmers University of Technology, Gothenburg SE-41296, Sweden

ARTICLE INFO

Keywords:
Biosensor
Genistein
Flavonoid
Isoflavone

ABSTRACT

Genistein, an isoflavone found mainly in legumes, has been shown to have numerous health benefits for humans. Therefore, there is substantial interest in producing it using microbial cell factories. To aid in screening for high genistein producing microbial strains, a cell-based biosensor for genistein was developed by repurposing the Gal4DBD-ERα-VP16 (GEV) transcriptional activator in *Saccharomyces cerevisiae*. In the presence of genistein, the GEV sensor protein binds to the *GAL1* promoter and activates transcription of a downstream GFP reporter. The performance of the biosensor, as measured by fold difference in GFP signal intensity after external genistein induction, was improved by engineering the sensor protein, its promoter and the reporter promoter. Biosensor performance increased when the weak promoter *REV1*p was used to drive GEV sensor gene expression and the VP16 transactivating domain on GEV was replaced with the tripartite VPR transactivator that had its NLS removed. The biosensor performance further improved when the binding sites for the inhibitor Mig1 were removed from and two additional Gal4p binding sites were added to the reporter promoter. After genistein induction, our improved biosensor output a GFP signal that was 20 times higher compared to the uninduced state. Out of the 8 flavonoids tested, the improved biosensor responded only to genistein and in a somewhat linear manner. The improved biosensor also responded to genistein produced *in vivo*, with the GFP reporter intensity directly proportional to intracellular genistein concentration. When combined with fluorescence-based cell sorting technology, this biosensor could facilitate high-throughput screening of a genistein-producing yeast cell factory.

1. Introduction

Genistein is a phytochemical prized for its medicinal properties. Clinically, it exhibits antioxidant, anti-inflammatory, anti-osteoclastic, anticancer, and anti-obesity activities [1–4]. Molecularly, genistein is similar to estradiol, the major endogenous estrogen in humans, and thus has seen substantial interest for use in hormone replacement therapy. Independent of its estrogenic activities, genistein has also been shown to inhibit the activities of topoisomerase II [5,6] and protein tyrosine kinases [7,8], which are master regulators that can either promote or inhibit the activities of many other receptors, enzymes and transcription factors [9,10]. Due to the multi-target nature of its molecular function, genistein has also been shown to have tumorigenic properties in certain tissues [11,12]. Vigorous studies are currently underway on how to best deploy genistein for therapeutic purposes.

Genistein belongs to a class of polyphenolic compounds called flavonoids. All flavonoids share a core polyphenolic ring structure but differ in their degree of saturation and oxidation, ring positioning and functional group substitution [13]. Found ubiquitously throughout the plant kingdom, flavonoids play important roles in different aspects of plant development, and in plant interactions with animals and microbes [14]. In legumes, genistein is primarily involved in promoting symbiotic relationships with rhizobial bacteria and in the defense against fungal pathogens [15–18]. Genistein is found abundantly in legumes such as soybean [19], but because soybean also produces many other flavonoids, purification of genistein results in co-extraction of a mixture of many different flavonoids. For pharmaceutical purposes, a pure product is often desired. An economical way to produce pure genistein is using synthetic biology and microbial cell factories.

Combined with our understanding of cell metabolism and biosynthetic pathways, we can use synthetic biology to design and construct novel biological parts and recombinant microorganisms to produce heterologous compounds. The key to making synthetic biology a viable manufacturing option is our ability to improve the performance of chosen cell factories. The improvement process usually involves reiterations of the design-build-test-learn process [20], with the testing step being the rate-limiting step in most cases as it usually involves target product extraction and measurement via an often low-throughput analytical method. A way to resolve this bottleneck is the development of metabolite biosensors. A metabolite biosensor detects the amount of a target molecule present and translates that information into a signal that is easily read by current cell sorting technologies. Principally, a biosensor

* Corresponding author.
E-mail address: siewers@chalmers.se (V. Siewers).
[#] These authors contributed equally to this work.

https://doi.org/10.1016/j.engmic.2023.100078
Received 1 December 2022; Received in revised form 25 January 2023; Accepted 29 January 2023
Available online 4 February 2023

consists of a sensor component possessing a high affinity towards the ligand of interest, and a reporter component, e.g. a fluorescent protein, that enables a simple and fast read-out. When built into a cell factory, a biosensor can dramatically increase the testing capacity, since a mixture of cells can be screened according to how much product is being made. The ability of cell factories to display their own metabolite concentration can greatly speed up the synthetic biology workflow [20,21].

Genistein has previously been synthesized from different precursors by microorganisms such as *Escherichia coli* and *Saccharomyces cerevisiae* [22–26]. To improve the performance of such cell factories, a biosensor would serve as a useful tool. A genistein-specific biosensor could potentially exploit the estrogenic nature of genistein. In mammals, estrogens such as estradiol exert their function via the estrogen receptors α and β (ERα, ERβ), which are intracellular hormone receptors that activate gene transcription in the presence of estrogens. Besides estrogens, many other estrogenic chemicals [e.g. dichlorodiphenyltrichloroethane (DDT), bisphenol A (BPA)], drugs [selective estrogen receptor modulators (SERMs)], and phytochemicals [e.g. coumestrol, equol, zearalenone, resveratrol, naringenin, kaempferol, daidzein, phloretin, quercetin and genistein] have been shown to bind to the ERs [27–29]. The human ERα localizes primarily to the nucleus. In the presence of its ligand, ligand binding induces a conformational change in the ligand binding domain (LBD) of the ERα that results in dimerization of ERα and subsequent transcriptional activation of target genes. The N-terminal half of ERα contains a constitutively active domain (AF-1), a DNA binding domain (DBD) and hinge region, with a nuclear localization signal (NLS) straddling the DBD and hinge region. The C-terminal half of ERα contains a ligand binding domain (LBD) [30–33]. Biologists have successfully used heterologously expressed human ERα in other organisms [34–36].

In *S. cerevisiae*, a chimeric protein has been engineered to consist of the human ERα ligand binding domain fused with the yeast Gal4 DNA binding domain (Gal4DBD), and the herpes simplex VP16 transcriptional activating domain (Fig. 1a). This chimeric protein is called GEV (Gal4DBD-ERα-VP16) [37]. Upon binding to estradiol, GEV translocates to the nucleus, where it binds to the yeast *GAL1* promoter and activates downstream gene expression (Fig. 1b) [38]. In yeast, GEV is a powerful tool for manipulating target gene expression because it induces a graded response that is proportional to the concentration of estradiol [39]. Since GEV contains the ligand binding domain of the ERα and ERα has also been found to respond to genistein, GEV should, in theory, be responsive to genistein in a graded manner.

In this study, we show that GEV does respond to genistein but not to other flavonoids that have been reported to interact with the ER [27,29], making it a highly selective biosensor applicable in *S. cerevisiae*. We improved the dynamic range of the biosensor from a 5- to a 20-fold signal increase upon genistein induction by engineering the transactivation domain of the sensor protein, its expression level, and the reporter promoter sequence. Finally, we demonstrate that the biosensor's operational range is in line with current genistein titers produced by yeast and can thus be used for measuring *in vivo* genistein production.

2. Materials and methods

2.1. Strains and plasmids

S. cerevisiae CEN.PK 113–11C was used as host strain for biosensor engineering and testing. *E. coli* DH5α was used for plasmid assembly and propagation. Engineered yeast strains, plasmids and primers used in this study are listed in Supplementary Tables S1–S3.

2.2. Media and culture conditions

Yeast Extract-Peptone-Dextrose (YPD) medium consisted of 20 g/L yeast peptone from meat, 10 g/L yeast extract and 20 g/L glucose. YPD with G418 (YPD+G418) was made by adding 200 mg/L geneticin (G418) to YPD; YPD with G418 and nourseothricin (YPD+G418+nourseothricin) was made by adding 200 mg/L G418 and 100 mg/mL nourseothricin to YPD. Synthetic defined uracil dropout medium (SD-URA) consisted of 0.77 g/L complete supplement mix without uracil, 6.9 g/L yeast nitrogen base without amino acids and 20 g/L glucose. SD medium with 5-fluoroorotic acid (5-FOA plates) was made by adding 1 g/L 5-fluoroorotic acid and 50 mg/L uracil to SD-URA. Plates of aforementioned media were made by adding 20 g/L agar. Complete supplement medium (CSM) medium consisted of 0.79 g/L complete supplement mix, 6.9 g/L yeast nitrogen base without amino acids and 20 g/L glucose. Delft medium [40], pH 4.5, consisted of 7.5 g/L $(NH_4)_2SO_4$, 14.4 g/L KH_2PO_4, 0.5 g/L $Mg_2SO_{4x}7H_2O$, 2 mL/L trace metals solution and 1 mL/L vitamin solution. The trace metal solution consisted of 4.5 g/L $CaCl_2{\cdot}2H_2O$, 4.5 g/L $ZnSO_4{\cdot}7H_2O$, 3 g/L $FeSO_4{\cdot}7H_2O$, 1 g/L H_3BO_3, 1 g/L $MnCl_2{\cdot}4H_2O$, 0.4 g/L $Na_2MoO_4{\cdot}2H_2O$, 0.3 g/L $CoCl_2{\cdot}6H_2O$, 0.3 g/L $CuSO_4{\cdot}5H_2O$, 0.1 g/L KI and 19 g/L $Na_2EDTA{\cdot}2H_2O$ and the vitamin solution consisted of 50 mg/L D-biotin, 200 mg/L *p*-aminobenzoic acid, 1 g/L nicotinic acid, 1 g/LD-pantothenic acid hemicalciumsalt, 1 g/L pyridoxine-HCl, 1 g/L thiamine-HCl and 25 g/L myo-inositol. Unless otherwise stated, yeast cultures were grown at 30 °C with 220 RPM shaking.

For *E. coli* cultivation, LB medium consisting of 10 g/L peptone from casein, 10 g/L NaCl and 5 g/L yeast extract was used. The pH was set to 7.0 using 5 M NaOH. Ampicillin was added at 100 mg/L for plasmid selection. Agar was added at 16 g/L to prepare solid media. *E. coli* cultures were grown at 37 °C with 180 RPM shaking.

Yeast nitrogen base, complete supplement mix and complete supplement mix without uracil were purchased from Formedium (Norfolk, UK). All other chemicals were purchased from Sigma-Aldrich/Merck (Darmstadt, Germany).

2.3. Whole-plasmid PCR

A new method for performing simple plasmid manipulation was developed during the course of this study. In this method, a pair of divergent primers harboring 20–30-mer overlapping regions at their 5′ ends were used to amplify the whole plasmid, as demonstrated in supplemental Fig. S1. For simple substitution or insertion, sequences to replace or be added were incorporated into primers at the 5′ overlapping region. For truncation, the 5′ overlapping region on each of the divergent primers contained approximately 10 bases immediately upstream and downstream of the truncation site such that there were around 20 bases of complementarity between the two primers. This method, which we named whole-plasmid PCR, relies on the processivity and fidelity of proofreading DNA polymerases, their lack of 5′ → 3′ exonuclease activity, and the ability of *E. coli* DH5α to perform simple homologous recombination *in vivo*. The workflow for whole-plasmid PCR involved 1) PCR amplification, 2) removal of template plasmid through DpnI digestion, and 3) direct *E. coli* transformation of unpurified reaction mix. For amplification, a 20 μL reaction mix containing 20 ng of template plasmid, 4 nmol of each dNTP, 10 pmol of each primer and 0.4 U Phusion HF DNA Polymerase (Thermo Fisher Scientific, Waltham, MA, USA) in 1X Phusion HF Buffer was prepared. The reaction mix was then cycled through the following steps: initial denaturation at 98 °C for 2 min; 20 cycles of 98 °C for 7 s, annealing temperature for 10 s, 72 °C for 30 s/kb plasmid; followed by final extension at 72 °C for 10 min. After amplification, 0.5 μL FastDigest DpnI was added directly to the PCR reaction mix and incubated at 37 °C for at least 1 h to digest the template plasmid. After DpnI digestion, 5 μL of unpurified reaction mix was added to 50 μL chemically competent *E. coli* DH5α [41] for transformation using a standard heat-shock protocol. Briefly, the transformation mix was incubated on ice for 30 min, followed by a 30 s incubation at 42 °C, then returned to ice for 2 min. Transformed cells were allowed to recover by adding 500 μL LB followed by shaking at 200 RPM, 37 °C for 1 h. After recovery, 100 μL of the mix was plated onto a prewarmed LB plate with appropriate selection marker. 2–3 colonies from

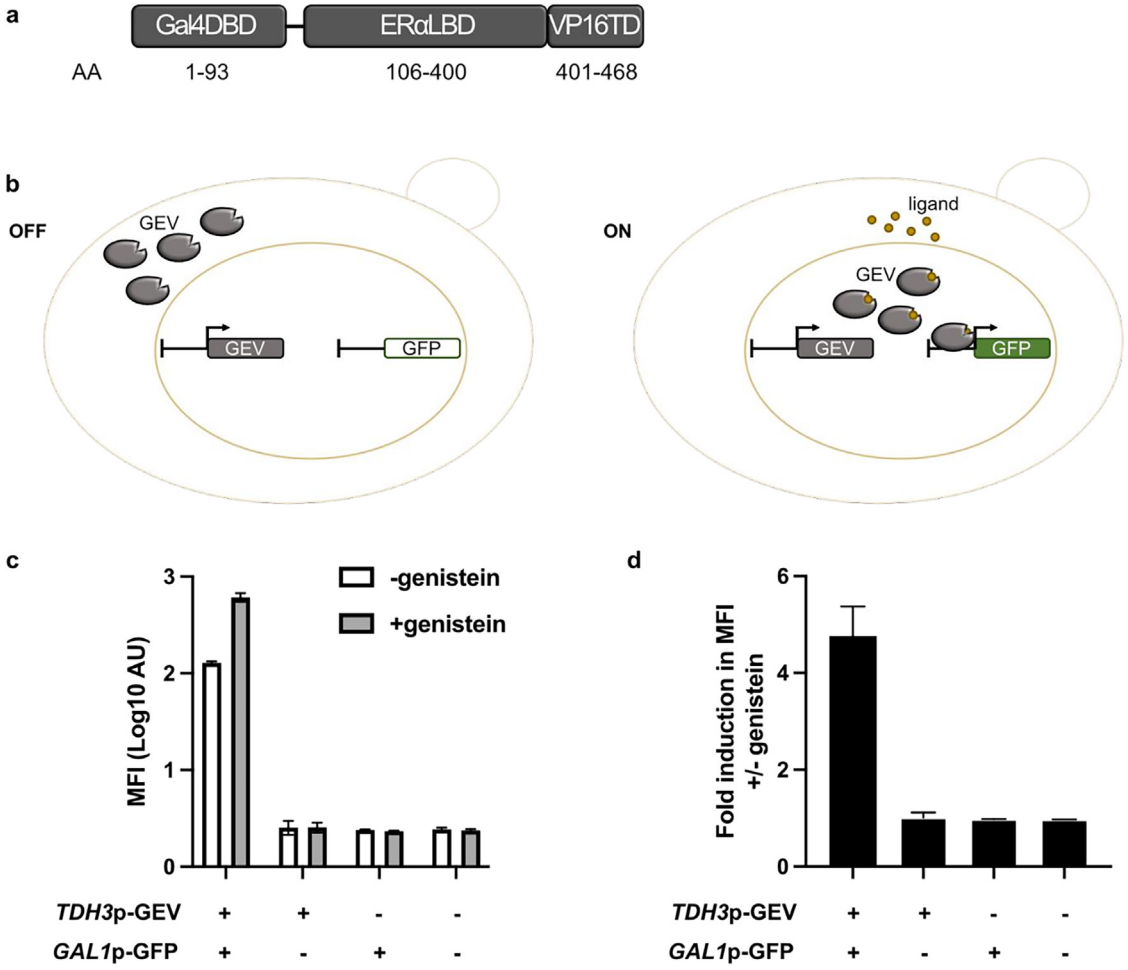

Fig. 1. Transcriptional activator GEV as genistein biosensor. (**a**) The GEV chimeric protein consists of the Gal4 DNA binding domain (Gal4DBD), Estrogen Receptor α ligand binding domain (ERαLBD) and VP16 transactivating domain (VP16TD). (**b**) Schematic illustration showing the proposed mechanism of GEV biosensor action based on its subcellular localization in the presence of estradiol [38]. Cytoplasmic GEV is translocated to the nucleus upon ligand binding. Ligand-bound nuclear GEV then binds to the *GAL1* promoter and activates downstream reporter transcription. (**c, d**) Median fluorescence intensity (MFI) values (**c**) and fold change in MFI upon genistein induction (**d**) of GEV biosensor strains based on GFP intensity measurement by flow cytometry. Cells were incubated with or without 100 μM genistein for 22 h. Values are shown as mean +/- s.d. from three biological replicates. AU, arbitrary units.

the transformation plate were picked and sequenced to verify successful plasmid manipulation. Small colonies should be avoided as they may contain concatemers. This method routinely yielded >90% correct plasmids and has been used to successfully manipulate plasmids as large as 10 kb.

Whole-plasmid PCR was successfully used to replace (e.g. exchange of gRNA encoding sequence in existing gRNA plasmids), add (e.g. adding short regulatory sequences), and remove sequences from a plasmid (e.g. NLS removal). One constraint is that the replacement sequence or added sequence needs to be short enough to fit on a custom oligonucleotide primer.

2.4. Yeast strain engineering

Unless otherwise stated, yeast genetic manipulation was performed using standard procedures [42,43]. Oligonucleotide primers were obtained from either Eurofins Genomics Germany GmbH (Ebersberg, Germany) or Integrated DNA Technologies (Coralville, IA, USA) and restriction enzymes were purchased from Thermo Fisher Scientific (Waltham, MA, USA). The GEV/GEVPR/GEVPR2 sequences, all reporter promoter sequences and genistein pathway gene sequences are given in the Supplementary.

A yeast strain harboring deletions in the *GAL4* coding sequence and the *GAL1–10* promoter was generated by sequential deletion of these loci using CRISPR/Cas9-mediated homologous recombination. For each deletion, an all-in-one plasmid encoding both Cas9 and target-specific gRNA was constructed by replacing the gRNA sequence of pECAS9-gRNA-KlURA3-tHFD1 (generated in [44]) using whole-plasmid PCR with primer pairs LC141/LC140 for targeting the *GAL4* ORF, or LC131/LC136 for targeting the *GAL1–10* promoter. The *S. cerevisiae* host strain was transformed with the plasmid together with a 120-mer repair fragment constructed by annealing complementary oligos LCF007/LCF008 for *GAL4* ORF deletion, or LCF003/LCF004 for the *GAL1–10* promoter. Successful transformants were selected based on growth on SD-URA plates. After transformation, genomic DNA was extracted and deletion was confirmed by PCR using primers LCD003/LCD004 for *GAL4* ORF deletion, or LCD001/LCD002 for *GAL1–10* promoter deletion. The CRISPR plasmid was removed by 5-FOA counter-selection before the next round of deletion or downstream use of the strain.

Strains expressing the GEV/GEVPR/GEVPR2 sensor protein and/or reporter protein were constructed by sequential gene integration using the EasyClone MarkerFree Toolkit [45]. All GEV/GEVPR/GEVPR2 sensor constructs were integrated into chromosomal locus X-4; all reporter constructs were integrated into chromosomal locus XI-1. Genistein pathway constructs were integrated into chromosomal locus XI-3. Integrative plasmids were assembled following the EasyClone MarkerFree manual with modifications described below.

To assemble the integrative plasmids for *TDH3*p-GEV-*CYC1*t and *TDH3*p-GEVPR-*CYC1*t integrations (pLC125 and pLC126, respectively), Gibson cloning (New England Biolabs, Ipswich, MA, USA) was performed using SfaAI/SacI-digested pCfB3035 as vector and PCR-amplified promoter and ORF fragments as inserts. *TDH3*p was amplified from pTS-38 [46] using primer pairs LC185/LC186. GEV was amplified from a custom synthetic DNA template (sequence provided in Supplementary) that was codon-optimized for expression in *S. cerevisiae* (Doulix, Explora Biotech, Venice, Italy), using primer pair LC191/LC192. GEVPR was amplified in two pieces: a fragment encoding Gal4DBD and ERLBD was amplified from aforementioned synthetic GEV template using LC191/LC204, and a fragment encoding VPR was amplified from dCas9V2 [47] using LC205/LC206. To generate the plasmid for *TDH3*p-GEVPR2-*CYC1*t integration, whole-plasmid PCR was performed using LC207/LC208 from pLC126 to remove the NLS. To assemble the integrative plasmids for *REV1*p-GEV-*CYC1*t, *REV1*p-GEVPR-*CYC1*t, *REV1*p-GEVPR2-*CYC1*t integration (pLC135, pLC151, pLC152, respectively), Gibson cloning was performed using SfaAI/SacI digested pCfB3035 as vector and PCR-amplified promoter and ORF fragments as inserts. The *REV1* promoter was amplified from CEN.PK 113–11C genomic DNA using LC247/LC248. GEV was amplified from pLC125 using LC249/192. GEVPR was amplified from pLC126 using LC249/206. GEVPR2 was amplified from pLC127 using LC249/LC206.

To assemble the plasmid for promoter A (pLC121) integration, Gibson cloning was performed using SfaAI/PstI-digested pCfB3036 as vector and PCR-amplified *GAL1* promoter and yeGFP ORF fragments as inserts. The native *GAL1* promoter was amplified from CEN.PK 113–11C genomic DNA using LC199/LC200. yeGFP was amplified from pTS-37 [46] using LC201/LC190.

To generate the plasmid for integrating promoter B (pLC155), whole-plasmid PCR was performed using LC267/LC268 from pLC121 to add the sequence *gta* upstream of the *GAL1* promoter.

To assemble plasmids for promoters C (pLC156) and G (pLC167) integration, Gibson cloning was used to replace the native *GAL1* promoter in pLC121 with promoter C or G. The *GAL1* promoter with deleted Mig1BS for promoter C was amplified using LC267/LC200. The 13X Gal4BS synthetic promoter G was amplified from pIOX179 using LC271/LC272 [48]. Although Joshi et al. stated that pIOX179 contained 10 Gal4 binding sites in their 2007 study, we found that the promoter actually contains 13 binding sites.

To generate plasmids for integrating promoters D, E and H, a 78-bp fragment containing 3XGal4BS flanked by BcuI sites was generated from primer extension of oligonucleotides LC269/LC270, and subcloned into pLC121, pLC155 and pLC156, respectively, following BcuI digestion. This was suitable because the Gal4BS sequence is palindromic. In addition to BcuI digestion, plasmid vectors were also treated with alkaline phosphatase (Thermo Fisher Scientific (Waltham, MA, USA)) to prevent self-ligation. Promoter F was from the same transformation reaction as promoter H but contained an unintended base change that destroyed the first Gal4BS. Given that it was our best-performing promoter, it was a serendipitous mistake stemming most likely from an error during oligonucleotide synthesis.

The genistein pathway genes were codon-optimized for *S. cerevisiae* and synthesized by GenScript Biotech (Piscataway Township, NJ, USA). A genistein pathway plasmid (pLC160) was generated with Gibson assembly, using XhoI/SacI-digested p416TEF [49] as vector, and PCR-amplified GmCPR, GmHID, TpIFS, promoters and terminators. The *CYC1* terminator used was present on the linearized vector. GmCPR was amplified using primers LC283/LC284. GmHID was amplified using primers LC289/LC290. TpIFS was amplified using primers LC279/LC280. The *ENO2* and *CCW12* promoters and the *TPI1* terminator were amplified from purified yeast genomic DNA using primers LC281/LC282, LC287/LC288 and LC291/LC292, respectively. The *TDH3* promoter was amplified from pTS38 [46] using primers LC293/LC186. The *ADH1* terminator was amplified from pLC155 using primers LC285/LC286. After bacterial transformation, plasmids were purified and sequenced. Note: Successful transformants produced small colonies.

The plasmid for genomic integration of (*TDH3*p-TpIFS-*CYC1*t)+(*CCW12*p-GmHID-*TPI*1t)+(*TEF1*p-GmCPR-*ADH1*t) (pDL091) was constructed by Gibson assembly using PstI/SacI digested vector pCfB2904 and PCR-amplified GmCPR, *TEF1* promoter and GmHID+TpIFS expression cassettes as inserts. GmCPR was amplified using primers DL372/DL373. *TEF1*p was amplified from genomic DNA using primers DL371/DL266. The GmHID and TpIFS expression cassettes including promoters and terminators were amplified from pLC160 using DL374/DL364.

The plasmids for integration of (*TDH3*p-GeIFS/GmIFS/MtIFS-*CYC1*t)+(*CCW12*p-GmHID-*TPI*1t)+(*TEF1*p-GmCPR-*ADH1*t) (pDL092–094) were constructed by Gibson assembly of two PCR-amplified DNA fragments into the SacI/SfaAI-digested vector pCfB2904. The GmHID and GmCPR expression cassettes were amplified from pDL091 using primers DL002 and DL371. GeIFS was amplified by DL360/DL361, GmIFS was amplified using DL362/363 and MtIFS was amplified by DL360/DL378 from synthesized templates.

Transformation was carried out according to the EasyClone MarkerFree manual with modifications. Briefly, the Cas9-encoding plasmid pCfB2312 was first used to transform *gal4*Δ *GAL1–10*pΔ cells, and the resulting strain was maintained as host. Next, an overnight preculture of host cells was diluted with 15 mL YPD+G418 to an OD_{600} of 0.2. The culture was allowed to grow for 6 h at 30 °C, 200 RPM to an OD_{600} of 1. Cells were pelleted and washed once with LiAc Mix (100 mM lithium acetate in TE) and resuspended in 180 μL LiAc Mix. For each transformation, 25 μL of resuspended cells were mixed with a 17-μL solution containing 1 μg of XbaI-linearized EasyClone integrative plasmid, 5 μg salmon sperm DNA and 250 ng gRNA helper plasmid. To this mixture, 200 μL PEG Mix (40% PEG 3350, 100 mM lithium acetate in TE) was added and mixed. The transformation mix was allowed to rest at 30 °C for 1 h before applying a heat shock at 42 °C for 20 min. The supernatant was removed after a 10 s spin, and the pellet was resuspended in 500 μL YPD. Cells were allowed to recover at 30 °C, 200 RPM for 1.5 h before plating on YPD+G418+nourseothricin. After transformation, genomic DNA was extracted and integration was confirmed via PCR according to the EasyClone MarkerFree manual. Confirmed transformants were grown in non-selective conditions to promote the removal of the Cas9-coding pCfB2312 and gRNA helper plasmid. Briefly, cells were cultivated in YPD for 2 days before streaking onto YPD plates. After 24-h growth on YPD, cells were replica-plated onto YPD+G418 and YPD+nourseothricin plates. Single colonies showing lack of growth on selective plates were restreaked onto new YPD plates. Removal of plasmids was confirmed by lack of growth on selective media prior to downstream processes.

2.5. Flow cytometry

Cells were grown in a Growth Profiler (Enzyscreen BV, Heemstede, the Netherlands) set at 30 °C and 250 RPM using 96-well Growth Profiler plates according to the manufacturer's instructions. Precultures were prepared by inoculation of 250 μL CSM. After overnight growth, 5 μL of precultures was added to 100 μL Delft medium supplemented with 2% glucose and 20 mg/L each of L-histidine HCl and uracil, then 5 μL of diluted cultures were added to 250 μL of the same medium. For flavonoid-induced cultures, flavonoid solution in DMSO was added to the medium to a final DMSO concentration of 2%, whereas DMSO without flavonoid was added to uninduced cultures. After 22 h growth, 1 μL of each culture was diluted into 200 μL PBS to arrest cell growth before loading onto a Guava® easyCyte™ flow cytometer (Luminex Corporation, s-Hertogenbosch, the Netherlands). GFP signal from 5000 detected cells per sample was measured with an excitation wavelength of 488 nm and a 525/30 BP filter. Raw data collected was analyzed using FlowJo version 10 software (FlowJo LLC, Ashland, OR, USA). Median intensity of the log-scale GFP fluorescence was used as the readout for analysis.

2.6. High-performance liquid chromatography (HPLC)

To measure intracellular metabolites, cell cultures were centrifuged at 4000 RPM for 10 min and the supernatant was removed. For total intra- and extracellular metabolite samples, the whole cell culture was used for sample preparation. Samples were freeze-dried for 48 h and metabolites were extracted with absolute ethanol by vortexing at high speed for 10 min. Samples were analyzed using a Dionex UltiMate 3000 HPLC (ThermoFisher Scientific, Waltham, MA, USA) connected to a UVD 340 U UV/VIS diode array detector (ThermoFisher Scientific, Waltham, MA, USA) and a Discovery^{TM} HS F5 column (15 cm x 4.6 mm, 5 μm particle size) (Sigma-Aldrich, St. Louis, MO, USA). A gradient elution program was used at a flow rate of 1.2 mL/min, using 10 mM ammonium formate, pH 3 (A) and acetonitrile (B). The eluent gradient started with 15% B (0–1.5 min), followed by an increase to 20% B (1.5–3 min), 25% B (3–24 min), 45% B (24–25 min), 50% B (25–27 min) and a final decrease to 15% B (27–28 min). Then, 10 μL of sample was injected into the column for each measurement. The column was set to 30 ˚C. Genistein and naringenin were detected at a wavelength of 280 nm at retention times of 13.8 min and 14.2 min, respectively. Analytical standards of naringenin were obtained from Sigma-Aldrich (St. Louis, MO, USA) and genistein was obtained from HWI group (Rülzheim, Germany).

3. Results and discussion

3.1. Transcriptional activator GEV as genistein biosensor

To test whether GEV could function as a genistein biosensor in yeast, its gene driven by the *TDH3* promoter (*TDH3*p-GEV) was integrated into the yeast genome along with a GFP reporter under the transcriptional control of the *GAL1* promoter (*GAL1*p-GFP). After 22 h of cultivation in media containing either no genistein or 100 μM genistein, cells were collected, and the median fluorescence intensity (MFI) was measured by flow cytometry. The fluorescence intensity of cells containing only the *TDH3*p-GEV sensor protein expression cassette or the *GAL1*p-GFP reporter expression cassette and wild-type cells were collected as control. Compared with the control cells, cells expressing both *TDH3*p-GEV and *GAL1*p-GFP had the highest background fluorescence without genistein induction. However, a significant increase in fluorescence signal was observed upon genistein addition only in cells containing both *TDH3*p-GEV and *GAL1*p-GFP (Fig. 1c). When the magnitude of increase was calculated by dividing the fluorescence intensity with genistein induction (100 μM) over fluorescence intensity without genistein induction (0 μM), there was a 5-fold increase observed only in cells containing the complete circuit (Fig. 1d). Taken together, GEV can function as a biosensor for genistein in yeast.

3.2. Genistein biosensor optimization through GEV protein engineering

We sought to improve the performance of our genistein biosensor by first engineering the GEV sensor protein. Since it was observed that the biosensor produced a high fluorescence signal in the absence of genistein, the first step towards optimization was to reduce the background fluorescence by decreasing the amount of GEV sensor protein in the cell. This was accomplished by replacing the strong constitutive *TDH3* promoter with a weaker *REV1* promoter [50]. Furthermore, to increase the sensitivity of the sensor protein, its ability to activate transcription was enhanced by replacing the VP16 transactivating domain of the GEV with a stronger transcriptional activator, VP64-p65-Rta (VPR) [51]. VPR contains VP64, four repeats of VP16 [52], p65, the transactivating domain of human RelA [53], and the transactivating domain of Rta, a transcriptional activator encoded by the Epstein-Barr virus [54]. Lastly, the NLS sequence that was embedded between VP64 and p65 in the original version of VPR was removed based on the importance of differential GEV nuclear translocation to its function. The Gal4-ER-VPR chimeric protein was given the name GEVPR. The version of GEVPR that had the NLS removed from VPR was given the name GEVPR2 (Fig. 2a). To test whether GEVPR and GEVPR2 were indeed improvements over GEV, all three versions of the sensor protein, driven by either the *TDH3* or the *REV1* promoter, were introduced into cells expressing the reporter *GAL1*p-GFP. Cells expressing different versions of the sensor protein without the *GAL1*p-GFP reporter were used as controls. After 22 h of cultivation in media containing either no genistein or 100 μM genistein, cells were collected, and the MFI was measured by flow cytometry (Fig. 2b). As expected, replacing the *TDH3* promoter with the *REV1* promoter reduced both background fluorescence and genistein-induced signal in GEV, GEVPR and GEVPR2; meanwhile, replacing VP16 with VPR increased both background and signal fluorescence when sensor protein expression was driven by either the *TDH3* or the *REV1* promoter. Surprisingly, removing the NLS sequence in VPR caused a decrease in both background and signal fluorescence only when sensor protein expression was driven by the *REV1* promoter. This could suggest that the NLS in VPR only plays a minor role in determining the localization of the chimeric transcription factor. The ERα LBD used in this study consists of amino acids 282–576 of the intact ERα and contains one of the three known ERα NLSs [55]. Although previous studies have shown that a truncated ERα containing only this NLS does not localize to the nucleus in either the presence or absence of a ligand, it is possible that this NLS can still facilitate nuclear localization in our chimeric protein [56,57]. These results might also indicate that mechanisms other than differential localization, for instance TF dimerization induced by ligand binding, could play a more important role in TF activation. To better understand how each version of the sensor protein affects the performance of the biosensor system, fold increases in fluorescence were calculated by dividing the MFI after genistein induction by the MFI without genistein induction. Overall, *REV1*p-GEVPR and *REV1*p-GEVPR2 outperformed other versions of the biosensor (Fig. 2c).

3.3. Genistein biosensor optimization through reporter promoter engineering

Next, we sought to further improve our biosensor by engineering the GFP reporter, focusing our efforts on the reporter promoter. For the reporter to respond to the Gal4DBD-containing GEV sensor protein, its expression was driven by the yeast native *GAL1* promoter (Fig. 3a, reporter A), which contains at its 5' end a cluster of three canonical Gal4 binding sites, a non-canonical Gal4 binding site and two binding sites for Mig1, a transcriptional regulator that inhibits the expression of certain *GAL* genes in the presence of glucose [58]. In addition to the core *GAL1* promoter, a previous study discovered that the bases GTA immediately upstream of the three canonical Gal4 binding sites are required for gene transcription by endogenous Gal4 [59]. Based on all this available knowledge on the *GAL1* promoter, several modifications to the core native promoter were tested: 1) extending the core promoter 25 bases upstream of the native *GAL1* promoter that included GTA bases; 2) removing Mig1 binding sites; and 3) adding multiple Gal4 binding sites 13 bases upstream of the native binding sites, with the additional Gal4 binding sites added 1–2 bases apart, mimicking the relative positions of Gal4 binding sites in the native *GAL1* promoter. These modifications and their different combinations (Fig. 3a, reporters B-F), along with a synthetic promoter containing 13 Gal4 binding sites (Fig. 3a, reporter G) [48] were tested in conjunction with the core native *GAL1* promoter to compare their effects on GFP signal intensity. For biosensor testing, all promoter-GFP variations were introduced into yeast strains containing either *REV1*p-GEVPR or *REV1*p-GEVPR2. Cells expressing the different versions of the promoter-GFP constructs without either *REV1*p-GEVPR or *REV1*p-GEVPR2 were used as controls. After 22 h of cultivation in media containing either no genistein or 100 μM genistein, cells were collected, and the MFI was measured by flow cytometry. Contrary to previous observations made with endogenous Gal4 transcription factor and *GAL1* promoter, the inclusion of bases GTA upstream of the *GAL1* promoter did not increase fluorescence intensity (Fig. 3b reporters B, C, E, F) [59]. A possible explanation for this discrepancy is that the reporter

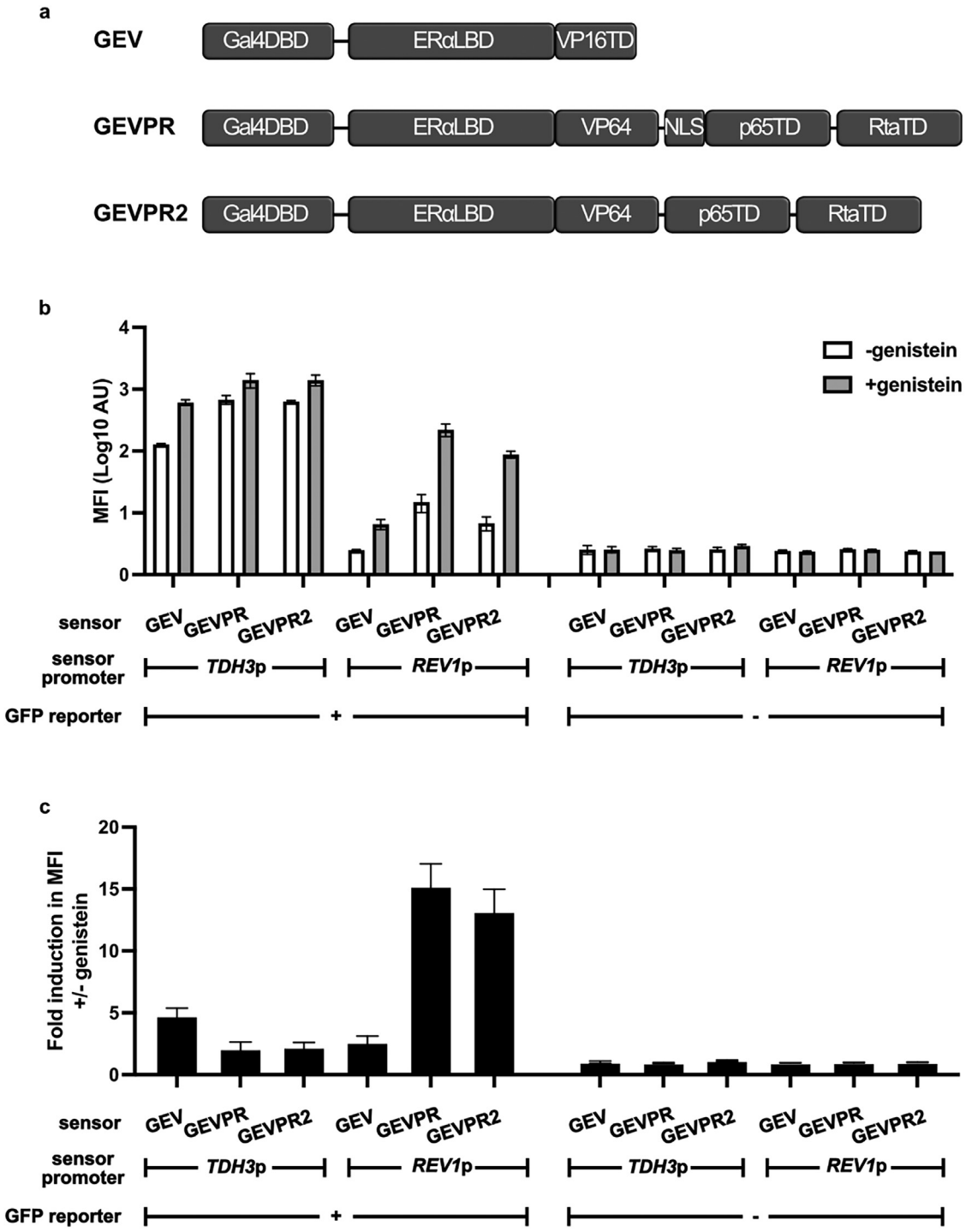

Fig. 2. Genistein biosensor optimization through GEV protein engineering. (**a**) Diagram comparing the domain composition of GEV, GEVPR and GEVPR2. (**b, c**) MFI values (**b**) and fold change in MFI upon genistein induction (**c**) of various genistein sensor strains based on GFP intensity measurement by flow cytometry. Genes encoding sensor proteins were driven by either a strong (*TDH3*p) or weak (*REV1*p) promoter. Cells were incubated with or without 100 μM genistein for 22 h. Values are shown as mean +/- s.d. from three biological replicates. AU, arbitrary units.

used in our study was integrated in a different site from the *ho* locus that was used in the previous study. As expected, removing Mig1 inhibitor binding sites increased both background and signal fluorescence (Fig. 3b reporters C, F). Interestingly, while having six Gal4 binding sites did not result in an increase in background and signal fluorescence, having five Gal4 binding sites did (Supplementary Fig. S2). Fortuitously, the promoter with five Gal4 binding sites came about because one of the cloning primers used harbored an error that abolished the first of the three upstream additional Gal4 binding sites. Finally, no fluorescence increase upon genistein induction was observed for the synthetic promoter containing 13 Gal4 binding sites. The synthetic promoter also produced the highest fluorescence in the absence of the sensor protein component. Besides the numerous Gal4 binding sites, this synthetic promoter used the *HIS3* promoter as core promoter instead of the *GAL1* promoter, leaving the possibility that factors other than GEVPR or GEVPR2 can activate transcription from the synthetic promoter (Fig. 3b reporter

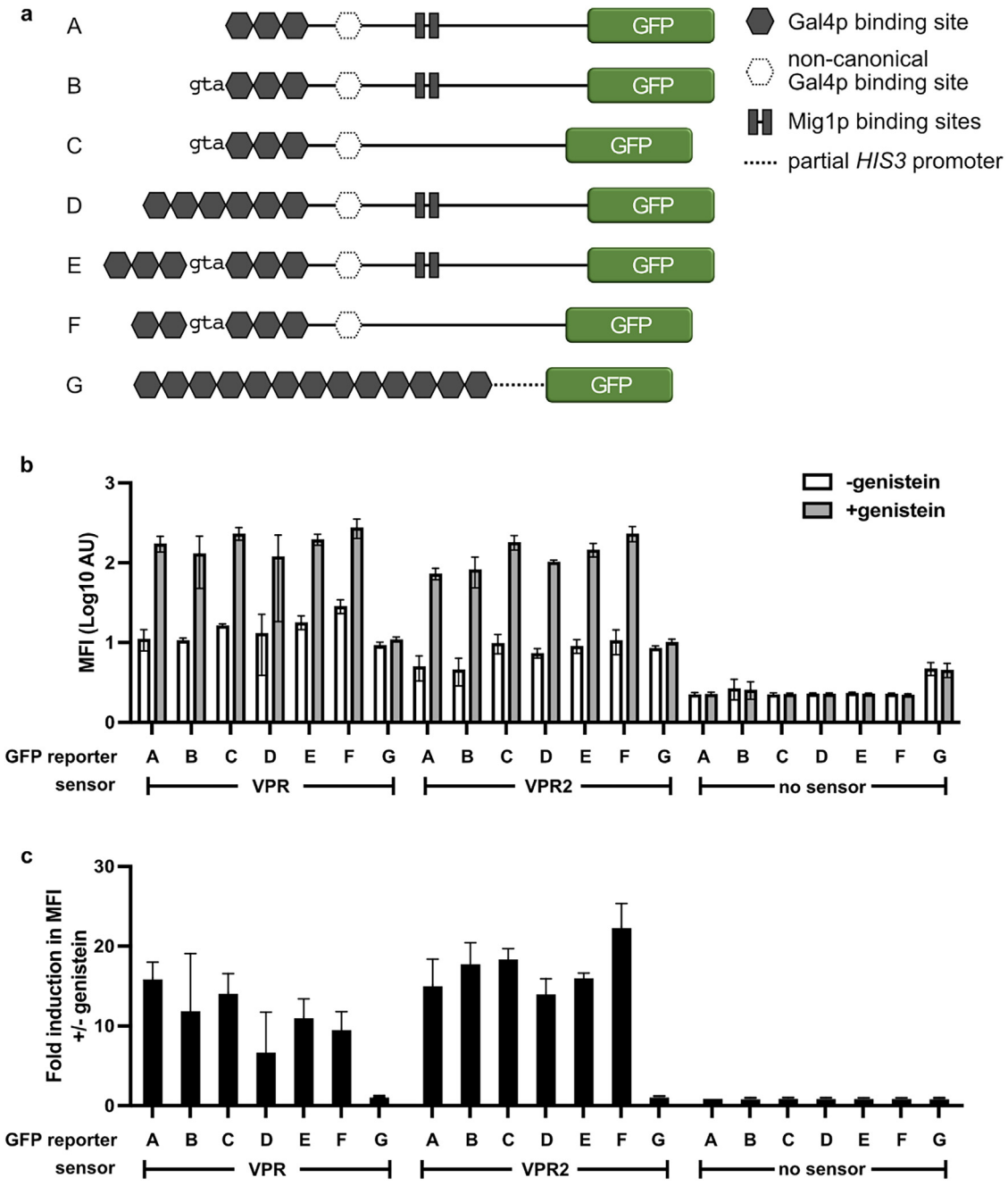

Fig. 3. Genistein biosensor optimization through reporter promoter engineering. (**a**) Schematic illustrations showing known motifs on the native *GAL1* promoter (A) and engineered variants (B-G). (**b, c**) MFI values (**b**) and fold change in MFI upon genistein induction (**c**) of various genistein biosensor strains based on GFP intensity measurement by flow cytometry. Genes encoding sensor proteins were driven by the weak *REV1* promoter. Cells were incubated with or without 100 μM genistein for 22 h. Values are shown as mean +/- s.d. from three biological replicates. AU, arbitrary units.

G). To tease out the best-performing reporter and sensor protein combination, the fold increase in fluorescence was calculated by dividing MFI after genistein induction by MFI without genistein induction. Overall, the biosensor using *REV1*p-GEVPR2 in combination with reporter F gave the highest fold change in reporter intensity upon genistein induction (Fig. 3c).

3.4. Determination of biosensor selectivity

Similarity in structure among flavonoids can potentially lead to specificity issues regarding the development of biosensors. To assess whether the sensor protein is specific to genistein, we tested our improved biosensor against several other flavonoids. These flavonoids were chosen because they are either precursors or possible by-products in the genistein synthesis pathway (naringenin chalcone, naringenin, phloretin) most structurally similar to genistein (daidzein), or known to trigger the ER (quercetin, kaempferol, daidzein, resveratrol) [27,29]. Including genistein, a total of 8 flavonoids were tested at the respective maximum concentration at which each flavonoid remained soluble in the media. As controls, cells expressing either the reporter or sensor protein alone were treated in parallel (Supplementary Fig. S3). After 22 h of cultivation in media containing the different flavonoids, cells were collected and the MFI was measured through flow cytometry. Out of the 8 flavonoids tested, genistein was the only flavonoid that elicited detectable signals from our biosensor (Fig. 4). Control cells containing either the reporter or sensor protein expression cassette alone

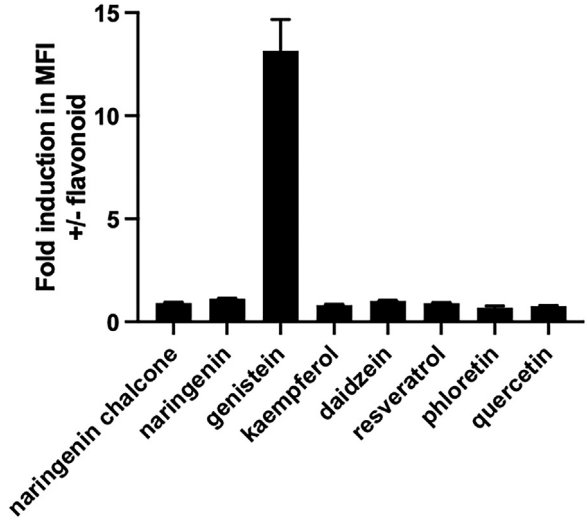

Fig. 4. Determination of biosensor specificity. Fold change in MFI after induction with various flavonoids. Flavonoids were tested at the highest concentrations at which they were soluble in growth media as determined empirically: 44 μM naringenin chalcone, 184 μM naringenin, 74 μM genistein, 18 μM kaempferol, 47 μM daidzein, 272 μM resveratrol, 365 μM phloretin, 66 μM quercetin. Cells were incubated in media containing flavonoids for 22 h. Values were calculated based on GFP intensity measurement by flow cytometry and are shown as mean +/- s.d. from three biological replicates.

did not show any significant fold increase in fluorescence upon treatment with each flavonoid. To our surprise, the biosensor did not respond to quercetin, kaempferol, daidzein or resveratrol, even though these flavonoids have been shown to trigger ERα [27,29]. One possibility is that genistein is structurally more estrogenic compared to other flavonoids. Indeed, Kuiper et al. performed solid-phase binding and solubilized receptor-ligand binding assays, which showed higher binding affinities of genistein (relative to 17β-estradiol) to both ERα and ERβ compared to daidzein, apigenin, kaempferol, quercetin, naringenin and phloretin [27]. Ligand-binding experiments by fluorescence polarization were performed by Mueller et al., showing that genistein also exhibits higher relative binding affinities to ERα/β than resveratrol [29]. Through luciferase activity assays in ERα or ERβ expressing human cell lines, genistein was further found to have stronger transactivation activities than other flavonoids tested [27,29]. Moreover, genistein can compete with estradiol for ER binding whereas quercetin for instance cannot [60]. Although these experiments were conducted under different conditions, they may explain why our GEV-based biosensor is highly specific to genistein. Along the same lines, the absence of induction signal from other flavonoids could also be due to the flavonoids being present in insufficient concentrations. Each flavonoid was tested at its maximal soluble concentration in our media. It is conceivable that these concentrations were not high enough for flavonoids to bind to ERα. Another possibility is that other flavonoids exert different effects on estrogen receptor functions compared to genistein. For example, the interaction of quercetin with ERα requires ER domains other than the ligand binding domain [60]. Perhaps the mechanism of interaction between ligand and receptor differs among flavonoids. Overall, our improved biosensor is sufficiently selective for most applications.

3.5. *Operational range characterization for the improved genistein biosensor*

For most applications, the biosensor needs to be able to not just detect the presence of the target molecule, but also report on its concentration. As an example, for an application such as high-throughput cell screening, a larger signal separation between concentrations means easier downstream sorting. To determine how well our improved biosensor can distinguish between different amounts of genistein, cells were grown in media containing increasing genistein concentrations. The same treatment was performed on cells containing the original GEV biosensor for comparison. After 22 h of cultivation in the genistein-containing media, cells were collected and the MFI was measured by flow cytometry. Both biosensor variants responded to concentrations as low as 2 μM. Although more genistein resulted in higher GFP signals in both strains, greater signal separation was observed with the improved variant. For example, the original biosensor measured an average MFI of 134 AU at 6 μM genistein and 654 AU at 100 μM genistein, whereas the improved biosensor measured an average MFI of 22 AU at 6 μM genistein and 217 AU at 100 μM genistein (Supplementary Fig. S4). This resulted in a 7-fold and a 16-fold increase in MFI for the original and improved biosensor, respectively (Fig. 5). In conclusion, the improved biosensor functions better at distinguishing between genistein concentrations. Concentrations above 100 μM could not be tested due to the limited solubility of genistein in media.

3.6. *Biosensor application for* in vivo *genistein production*

The goal for developing this biosensor was to be able to distinguish yeast strains producing different amounts of genistein. In plants, genistein is synthesized from the flavonoid naringenin via a two-step process: hydroxylation and concurrent aryl ring migration, followed by dehydration and double bond formation. The hydroxylation and ring migration step is catalyzed by isoflavone synthase (IFS), a cytochrome P450 monooxygenase that requires a cytochrome P450 reductase (CPR) for electron supply. The dehydration and double bond formation step can occur spontaneously but is facilitated by 2-hydroxyisoflavanone dehydratase (HID) in plants (Fig. 6a) [22]. When plant IFS genes from *Glycine max* (GmIFS), *Glycyrrhiza echinata* (GeIFS) or *Medicago truncatula* (MtIFS), and CPR and HID from *G. max* (GmCPR, GmHID) were introduced into our improved biosensor strain, the amount of genistein

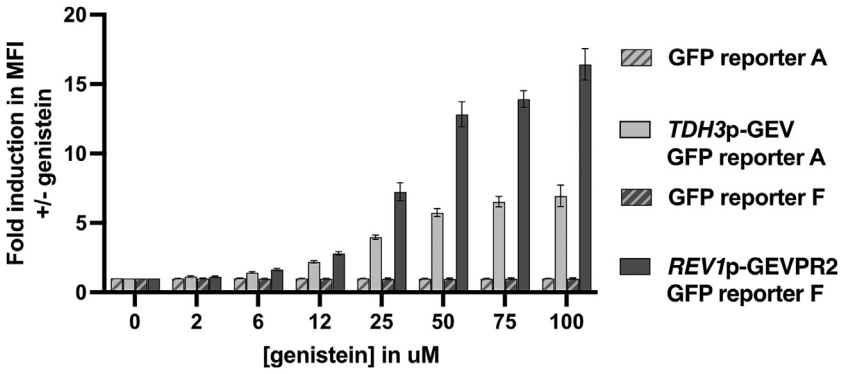

Fig. 5. Operational range characterization for the improved genistein biosensor. Fold changes in MFI upon induction with increasing genistein concentrations based on GFP intensity measurement by flow cytometry. Comparison is made between the best-performing biosensor strain (solid dark gray bar) and the original biosensor (solid light gray bar). Reporter only controls for each strain (striped bars). Cells were incubated with or without indicated concentration of genistein for 22 h. Values are shown as mean +/- s.d. from three biological replicates.

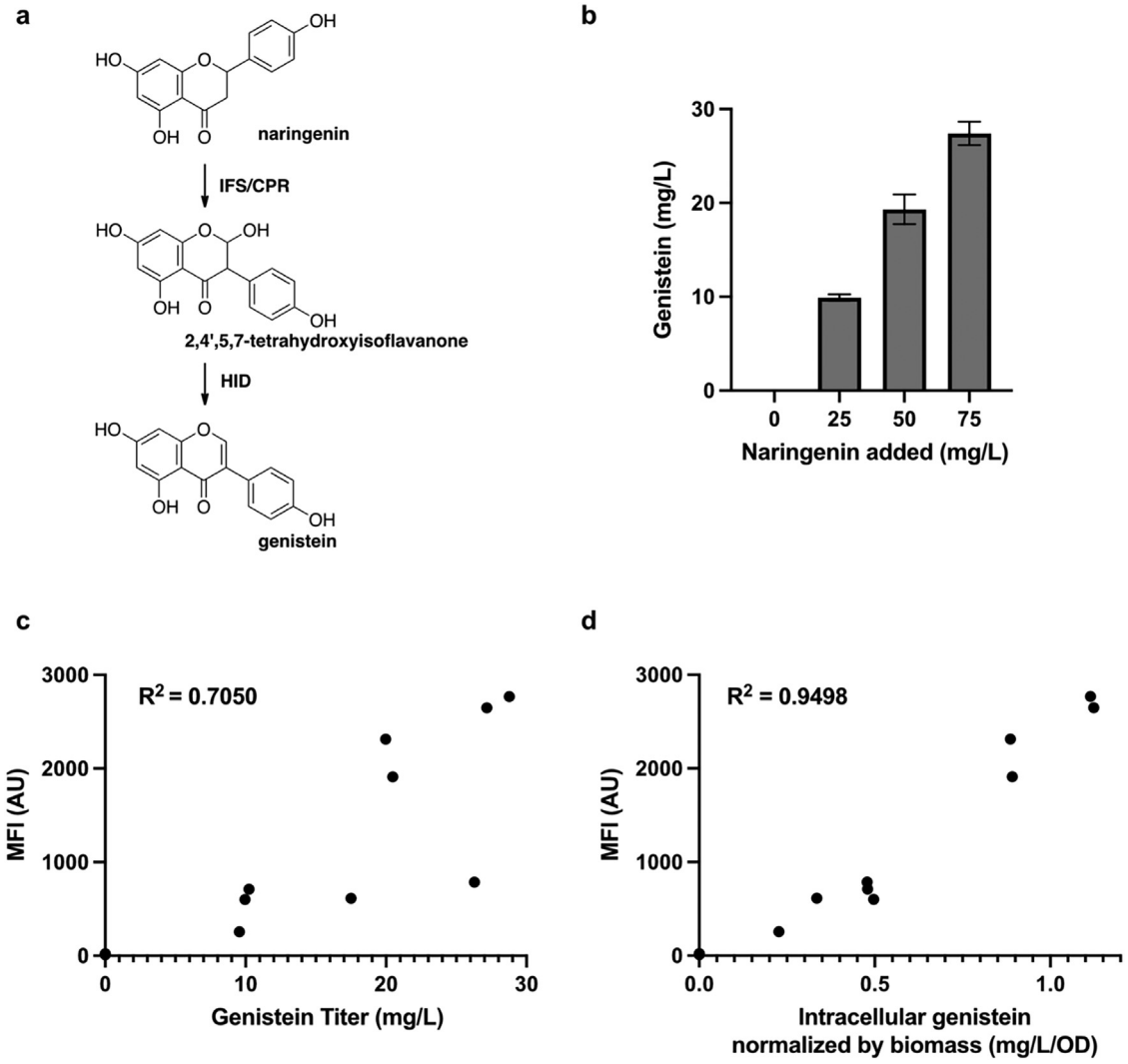

Fig. 6. Biosensor application for *in vivo* genistein production. (**a**) Schematic representation of heterologous genistein synthesis from naringenin [22]. Enzymes used are IFS, CPR and HID originating from *G. max*. (**b**) After 22 h cultivation of yGEN06 in media containing stated naringenin concentration, the genistein titer was measured using HPLC. (**c, d**) After 22 h cultivation of yGEN06 in media containing different naringenin concentrations, fluorescence intensity was detected by flow cytometry and total genistein titer (**c**) and intracellular genistein amount (**d**) were detected by HPLC. The intracellular genistein amount was normalized to culture OD.

produced corresponded with the naringenin concentration added to the media (Fig. 6b). While the GmIFS expressing strain produced the highest amount of genistein (Fig. S5), *Trifolium pratense* IFS, which was reported to have the highest activity in *S. cerevisiae*, did not produce any genistein in our strain (data not shown). By measuring both fluorescence intensity and genistein amount, one could test how well the biosensor signal correlated with the level of genistein production. After cells were incubated for 22 h in media containing different concentrations of naringenin, the median fluorescence intensity was measured by flow cytometry, and the total intra- and extracellular genistein titer was measured by HPLC. A biosensor strain without expression of IFS, CPR and HID was included as control to confirm that naringenin itself does not induce GFP expression (data not shown). In general, a higher genistein titer resulted in a higher GFP signal within each replicate, but the correlation was not consistent across replicates (Fig. 6c). We argue that what the sensor protein actually detects, is the intracellular genistein level. When compared to intracellular genistein level, the GFP signal was found to be in good correlation at R^2= 0.9498 (Fig. 6d). We conclude that our improved biosensor responds in a consistent, linear fashion to intracellular genistein levels.

4. Conclusion

In this work, we developed a highly specific genistein biosensor in *S. cerevisiae* based on the previously developed GEV transcriptional activator. The maximum dynamic range of the biosensor was expanded from 5- to 20-fold by rational engineering of different aspects of the sensor protein/reporter design. We further determined an operational range of 2–100 μM (with higher concentrations being limited by genistein solubility in media) and confirmed the applicability of the biosensor for intracellular genistein detection. For future optimization one might consider exploring other DNA and ligand binding domains for the sensor protein that may provide even higher affinities or improved orthogonality. For instance, exchanging the Gal4DBD for a heterologous one like the bacterial LexA DBD [61,62] could avoid off-target activation of endogenous Gal4-regulated genes and permit biosensor application in galactose-containing medium. In addition to ERα, genistein has also been reported to trigger ERβ, the other estrogen receptor in humans. ERβ has a higher affinity for genistein (0.86%) compared to ERα (0.032%) relative to estradiol [63]. Therefore, replacing the LBD of GEVPR2 with the LBD of ERβ could in

theory produce a biosensor that is more sensitive to low levels of genistein.

Biosensors have the potential to expedite the test phase of the design-build-test-learn cycle by facilitating microbial cell factory screening and thus shortening the overall time required for the development of a novel production process. Taken together, we think that our sensor can aid in the development of a genistein-producing *S. cerevisiae* strain.

Declaration of Competing Interest

The authors declare that they have no known competing financial interests or personal relationships that could have appeared to influence the work reported in this paper.

Acknowledgements

The authors thank the Sadowski laboratory for sharing pIOX179.This project received funding from the *European Union's Horizon 2020 research and innovation program* under grant agreement no. 814650.

Supplementary materials

Supplementary material associated with this article can be found, in the online version, at doi:10.1016/j.engmic.2023.100078.

References

[1] S. Banerjee, Y. Li, Z. Wang, F.H. Sarkar, Multi-targeted therapy of cancer by genistein, Cancer Lett. 269 (2) (2008) 226–242, doi:10.1016/j.canlet.2008.03.052.
[2] N. Behloul, G. Wu, Genistein: a promising therapeutic agent for obesity and diabetes treatment, Eur. J. Pharmacol. 698 (1) (2013) 31–38, doi:10.1016/j.ejphar.2012.11.013.
[3] G. Bhattarai, S.B. Poudel, S.H. Kook, J.C. Lee, Anti-inflammatory, anti-osteoclastic, and antioxidant activities of genistein protect against alveolar bone loss and periodontal tissue degradation in a mouse model of periodontitis, J. Biomed. Mater. Res. A 105 (9) (2017) 2510–2521, doi:10.1002/jbm.a.36109.
[4] H.S. Tuli, M.J. Tuorkey, F. Thakral, K. Sak, M. Kumar, A.K. Sharma, U. Sharma, A. Jain, V. Aggarwal, A. Bishayee, Molecular mechanisms of action of genistein in cancer: recent advances, Front. Pharmacol. 10 (1336) (2019), doi:10.3389/fphar.2019.01336.
[5] J. Markovits, C. Linassier, P. Fossé, J. Couprie, J. Pierre, A. Jacquemin-Sablon, J.M. Saucier, J.B.L. Pecq, A.K. Larsen, Inhibitory effects of the tyrosine kinase inhibitor genistein on mammalian DNA topoisomerase II, Cancer Res. 49 (18) (1989) 5111–5117.
[6] Y. Mizushina, K. Shiomi, I. Kuriyama, Y. Takahashi, H. Yoshida, Inhibitory effects of a major soy isoflavone, genistein, on human DNA topoisomerase II activity and cancer cell proliferation, Int. J. Oncol. 43 (4) (2013) 1117–1124, doi:10.3892/ijo.2013.2032.
[7] T. Akiyama, J. Ishida, S. Nakagawa, H. Ogawara, S. Watanabe, N. Itoh, M. Shibuya, Y. Fukami, Genistein, a specific inhibitor of tyrosine-specific protein kinases, J. Biol. Chem. 262 (12) (1987) 5592–5595, doi:10.1016/S0021-9258(18)45614-1.
[8] A. Levitzki, A. Gazit, Tyrosine kinase inhibition: an approach to drug development, Science 267 (5205) (1995) 1782–1788, doi:10.1126/science.7892601.
[9] S.R. Hubbard, J.H. Till, Protein tyrosine kinase structure and function, Annu. Rev. Biochem. 69 (1) (2000) 373–398, doi:10.1146/annurev.biochem.69.1.373.
[10] J.L. Nitiss, DNA topoisomerase II and its growing repertoire of biological functions, Nat. Rev. Cancer 9 (5) (2009) 327–337, doi:10.1038/nrc2608.
[11] L. Hilakivi-Clarke, E. Cho, I. Onojafe, M. Raygada, R. Clarke, Maternal exposure to genistein during pregnancy increases carcinogen-induced mammary tumorigenesis in female rat offspring, Oncol. Rep. 6 (5) (1999) 1089–1184, doi:10.3892/or.6.5.1089.
[12] P. Kijkuokool, I.S. Parhar, S. Malaivijitnond, Genistein enhances N-nitrosomethylurea-induced rat mammary tumorigenesis, Cancer Lett. 242 (1) (2006) 53–59, doi:10.1016/j.canlet.2005.10.033.
[13] A.N. Panche, A.D. Diwan, S.R. Chandra, Flavonoids: an overview, J. Nutr. Sci. 5 (2016), doi:10.1017/jns.2016.41.
[14] Mathesius, U., Flavonoid functions in plants and their interactions with other organisms, Plants 7 (2) (2018), 10.3390/plants7020030.
[15] L.V. Modolo, F.Q. Cunha, M.R. Braga, I. Salgado, Nitric oxide synthase-mediated phytoalexin accumulation in soybean cotyledons in response to the *Diaporthe phaseolorumf*. sp. *meridionalis* elicitor, Plant Physiol. 130 (3) (2002) 1288–1297, doi:10.1104/pp.005850.
[16] S.G. Pueppke, The genetic and biochemical basis for nodulation of legumes by rhizobia, Crit. Rev. Biotechnol. 16 (1) (1996) 1–51, doi:10.3109/07388559609146599.
[17] L.I. Rivera-Vargas, A.F. Schmitthenner, T.L. Graham, Soybean flavonoid effects on and metabolism by *Phytophthora sojae*, Phytochemistry 32 (4) (1993) 851–857, doi:10.1016/0031-9422(93)85219-H.
[18] P. van Rhijn, J. Vanderleyden, The *Rhizobium*-plant symbiosis, Microbiol. Rev. 59 (1) (1995) 124–142, doi:10.1128/mr.59.1.124-142.1995.
[19] P.B. Kaufman, J.A. Duke, H. Brielmann, J. Boik, J.E. Hoyt, A comparative survey of leguminous plants as sources of the isoflavones, genistein and daidzein: implications for human nutrition and health, J. Altern. Complement. Med. 3 (1) (1997) 7–12, doi:10.1089/acm.1997.3.7.
[20] J. Nielsen, J.D. Keasling, Engineering cellular metabolism, Cell 164 (6) (2016) 1185–1197, doi:10.1016/j.cell.2016.02.004.
[21] J.K. Rogers, N.D. Taylor, G.M. Church, Biosensor-based engineering of biosynthetic pathways, Curr. Opin. Biotechnol. 42 (2016) 84–91, doi:10.1016/j.copbio.2016.03.005.
[22] J.A. Chemler, C.G. Lim, J.L. Daiss, M.A.G. Koffas, A versatile microbial system for biosynthesis of novel polyphenols with altered estrogen receptor binding activity, Chem. Biol. 17 (4) (2010) 392–401, doi:10.1016/j.chembiol.2010.03.010.
[23] Y. Katsuyama, I. Miyahisa, N. Funa, S. Horinouchi, One-pot synthesis of genistein from tyrosine by coincubation of genetically engineered *Escherichia coli* and *Saccharomyces cerevisiae* cells, Appl. Microbiol. Biotechnol. 73 (5) (2007) 1143–1149, doi:10.1007/s00253-006-0568-2.
[24] E. Trantas, N. Panopoulos, F. Ververidis, Metabolic engineering of the complete pathway leading to heterologous biosynthesis of various flavonoids and stilbenoids in *Saccharomyces cerevisiae*, Metab. Eng. 11 (6) (2009) 355–366, doi:10.1016/j.ymben.2009.07.004.
[25] X. Liu, L. Li, G.R. Zhao, Systems metabolic engineering of *Escherichia coli* coculture for De Novo Production of genistein, ACS Synth. Biol. 11 (5) (2022) 1746–1757, doi:10.1021/acssynbio.1c00590.
[26] Meng, Y., Liu, X., Zhang, L., Zhao, G.R., Modular engineering of *Saccharomyces cerevisiae* for De Novo biosynthesis of genistein, Microorganisms 10 (7) (2022) 1402, doi:10.3390/microorganisms10071402.
[27] G.G.J.M. Kuiper, J.G. Lemmen, B. Carlsson, J.C. Corton, S.H. Safe, P.T. van der Saag, B. van der Burg, J.Å. Gustafsson, Interaction of estrogenic chemicals and phytoestrogens with estrogen receptor β, Endocrinology 139 (10) (1998) 4252–4263, doi:10.1210/endo.139.10.6216.
[28] B.H. Mitlak, F.J. Cohen, Selective estrogen receptor modulators, Drugs 57 (5) (1999) 653–663, doi:10.2165/00003495-199957050-00001.
[29] S.O. Mueller, S. Simon, K. Chae, M. Metzler, K.S. Korach, Phytoestrogens and their human metabolites show distinct agonistic and antagonistic properties on estrogen receptor α (ERα) and ERβ in human cells, Toxicol. Sci. 80 (1) (2004) 14–25, doi:10.1093/toxsci/kfh259.
[30] W. Huang, Y. Peng, J. Kiselar, X. Zhao, A. Albaqami, D. Mendez, Y. Chen, S. Chakravarthy, S. Gupta, C. Ralston, H.Y. Kao, M.R. Chance, S. Yang, Multidomain architecture of estrogen receptor reveals interfacial cross-talk between its DNA-binding and ligand-binding domains, Nat. Commun. 9 (1) (2018) 3520, doi:10.1038/s41467-018-06034-2.
[31] V. Kumar, S. Green, G. Stack, M. Berry, J.R. Jin, P. Chambon, Functional domains of the human estrogen receptor, Cell 51 (6) (1987) 941–951, doi:10.1016/0092-8674(87)90581-2.
[32] M. Parker, N. Arbuckle, S. Dauvois, P. Danielian, R. White, Structure and function of the estrogen receptor, Ann. NY Acad. Sci. 684 (1) (1993) 119–126.
[33] T. Moriyama, Y. Yoneda, M. Oka, M. Yamada, Transportin-2 plays a critical role in nucleocytoplasmic shuttling of oestrogen receptor-α, Sci. Rep. 10 (1) (2020) 18640, doi:10.1038/s41598-020-75631-3.
[34] S. Braselmann, P. Graninger, M. Busslinger, A selective transcriptional induction system for mammalian cells based on Gal4-estrogen receptor fusion proteins, PNAS 90 (5) (1993) 1657–1661, doi:10.1073/pnas.90.5.1657.
[35] C. Derntl, R. Mach, A. Mach-Aigner, Application of the human estrogen receptor within a synthetic transcription factor in *Trichoderma reesei*, Fungal Biol. Biotechnol. 7 (1) (2020) 12, doi:10.1186/s40694-020-00102-3.
[36] J. Zuo, Q.W. Niu, N.H. Chua, An estrogen receptor-based transactivator XVE mediates highly inducible gene expression in transgenic plants, Plant J. 24 (2) (2000) 265–273, doi:10.1046/j.1365-313x.2000.00868.x.
[37] C.Y. Gao, J.L. Pinkham, Tightly regulated, beta-estradiol dose-dependent expression system for yeast, Biotechniques 29 (6) (2000) 1226–1231, doi:10.2144/00296st02.
[38] R.S. McIsaac, S.J. Silverman, M.N. McClean, P.A. Gibney, J. Macinskas, M.J. Hickman, A.A. Petti, D. Botstein, Fast-acting and nearly gratuitous induction of gene expression and protein depletion in *Saccharomyces cerevisiae*, Mol. Biol. Cell 22 (22) (2011) 4447–4459, doi:10.1091/mbc.E11-05-0466.
[39] S. Takahashi, P.M. Pryciak, Membrane localization of scaffold proteins promotes graded signaling in the yeast MAP kinase cascade, Curr. Biol. 18 (16) (2008) 1184–1191, doi:10.1016/j.cub.2008.07.050.
[40] N.B. Jensen, T. Strucko, K.R. Kildegaard, F. David, J. Maury, U.H. Mortensen, J. Forster, J. Nielsen, I. Borodina, EasyClone: method for iterative chromosomal integration of multiple genes in *Saccharomyces cerevisiae*, FEMS Yeast Res. 14 (2) (2014) 238–248, doi:10.1111/1567-1364.12118.
[41] H. Inoue, H. Nojima, H. Okayama, High efficiency transformation of *Escherichia coli* with plasmids, Gene 96 (1) (1990) 23–28, doi:10.1016/0378-1119(90)90336-p.
[42] R. Rothstein, Targeting, disruption, replacement, and allele rescue: integrative DNA transformation in yeast, Methods Enzymol. 194 (1991) 281–301, doi:10.1016/0076-6879(91)94022-5.
[43] F. Sherman, Getting started with yeast, Methods Enzymol. 350 (2002) 3–41, doi:10.1016/S0076-6879(02)50954-X.
[44] Z. Zhu, Y.J. Zhou, M.K. Kang, A. Krivoruchko, N.A. Buijs, J. Nielsen, Enabling the synthesis of medium chain alkanes and 1-alkenes in yeast, Metab. Eng. 44 (2017) 81–88, doi:10.1016/j.ymben.2017.09.007.
[45] M.M. Jessop-Fabre, T. Jakočiūnas, V. Stovicek, Z. Dai, M.K. Jensen, J.D. Keasling, I. Borodina, EasyClone-MarkerFree: a vector toolkit for marker-less integration of genes into *Saccharomyces cerevisiae* via CRISPR-Cas9, Biotechnol. J. 11 (8) (2016) 1110–1117, doi:10.1002/biot.201600147.

[46] M.L. Skjoedt, T. Snoek, K.R. Kildegaard, D. Arsovska, M. Eichenberger, T.J. Goedecke, A.S. Rajkumar, J. Zhang, M. Kristensen, B.J. Lehka, S. Siedler, I. Borodina, M.K. Jensen, J.D. Keasling, Engineering prokaryotic transcriptional activators as metabolite biosensors in yeast, Nat. Chem. Biol. 12 (11) (2016) 951–958, doi:10.1038/nchembio.2177.

[47] R. Ferreira, C. Skrekas, J. Nielsen, F. David, Multiplexed CRISPR/Cas9 genome editing and gene regulation using Csy4 in *Saccharomyces cerevisiae*, ACS Synth. Biol. 7 (1) (2018) 10–15, doi:10.1021/acssynbio.7b00259.

[48] P.B. Joshi, M. Hirst, T. Malcolm, J. Parent, D. Mitchell, K. Lund, I. Sadowski, Identification of protein interaction antagonists using the repressed transactivator two-hybrid system, Biotechniques 42 (5) (2007) 635–644, doi:10.2144/000112434.

[49] D. Mumberg, R. Müller, M. Funk, Yeast vectors for the controlled expression of heterologous proteins in different genetic backgrounds, Gene 156 (1) (1995) 119–122, doi:10.1016/0378-1119(95)00037-7.

[50] M.E. Lee, A. Aswani, A.S. Han, C.J. Tomlin, J.E. Dueber, Expression-level optimization of a multi-enzyme pathway in the absence of a high-throughput assay, Nucleic Acids Res. 41 (22) (2013) 10668–10678, doi:10.1093/nar/gkt809.

[51] A. Chavez, J. Scheiman, S. Vora, B.W. Pruitt, M. Tuttle, P.R.I. E, S. Lin, S. Kiani, C.D. Guzman, D.J. Wiegand, D. Ter-Ovanesyan, J.L. Braff, N. Davidsohn, B.E. Housden, N. Perrimon, R. Weiss, J. Aach, J.J. Collins, G.M. Church, Highly efficient Cas9-mediated transcriptional programming, Nat. Methods 12 (4) (2015) 326–328, doi:10.1038/nmeth.3312.

[52] R.R. Beerli, D.J. Segal, B. Dreier, C.F. Barbas 3rd, Toward controlling gene expression at will: specific regulation of the erbB-2/HER-2 promoter by using polydactyl zinc finger proteins constructed from modular building blocks, PNAS 95 (25) (1998) 14628–14633, doi:10.1073/pnas.95.25.14628.

[53] J.M. O'Shea, N.D. Perkins, Regulation of the RelA (p65) transactivation domain, Biochem. Soc. Trans. 36 (4) (2008) 603–608, doi:10.1042/BST0360603.

[54] J.M. Hardwick, L. Tse, N. Applegren, J. Nicholas, M.A. Veliuona, The Epstein-Barr virus R transactivator (Rta) contains a complex, potent activation domain with properties different from those of VP16, J. Virol. 66 (9) (1992) 5500–5508, doi:10.1128/jvi.66.9.5500-5508.19.

[55] A. Guiochon-Mantel, P. Lescop, S. Christin-Maitre, H. Loosfelt, M. Perrot-Applanat, E. Milgrom, Nucleocytoplasmic shuttling of the progesterone receptor, EMBO J. 10 (12) (1991) 3851–3859, doi:10.1002/j.1460-2075.1991.tb04954.x.

[56] M. Lombardi, G. Castoria, A. Migliaccio, M.V. Barone, R. Di Stasio, A. Ciociola, D. Bottero, H. Yamaguchi, E. Appella, F. Auricchio, Hormone-dependent nuclear export of estradiol receptor and DNA synthesis in breast cancer cells, J. Cell Biol. 182 (2) (2008) 327–340, doi:10.1083/jcb.200712125.

[57] T. Ylikomi, M.T. Bocquel, M. Berry, H. Gronemeyer, P. Chambon, Cooperation of proto-signals for nuclear accumulation of estrogen and progesterone receptors, EMBO J. 11 (10) (1992) 3681–3694, doi:10.1002/j.1460-2075.1992.tb05453.x.

[58] J.O. Nehlin, M. Carlberg, H. Ronne, Control of yeast GAL genes by MIG1 repressor: a transcriptional cascade in the glucose response, EMBO J. 10 (11) (1991) 3373–3377, doi:10.1002/j.1460-2075.1991.tb04901.x.

[59] G.L. Elison, Y. Xue, R. Song, M. Acar, Insights into bidirectional gene expression control using the canonical GAL1/GAL10 promoter, Cell Rep. 25 (3) (2018) 737–748, doi:10.1016/j.celrep.2018.09.050.

[60] P. Miodini, L. Fioravanti, G.D. Fronzo, V. Cappelletti, The two phyto-oestrogens genistein and quercetin exert different effects on oestrogen receptor function, Br. J. Cancer 80 (8) (1999) 1150–1155, doi:10.1038/sj.bjc.6690479.

[61] T. Zhou, Z. Liang, M.A. Marchisio, Engineering a two-gene system to operate as a highly sensitive biosensor or a sharp switch upon induction with β-estradiol, Sci. Rep. 12 (2022) 21791, doi:10.1038/s41598-022-26195-x.

[62] D.S.M. Ottoz, F. Rudolf, J. Stelling, Inducible, tightly regulated and growth condition-independent transcription factor in *Saccharomyces cerevisiae*, Nucleic Acids Res. 42 (17) (2014) e130, doi:10.1093/nar/gku616.

[63] A. Escande, A. Pillon, N. Servant, J.P. Cravedi, F. Larrea, P. Muhn, J.C. Nicolas, V. Cavaillès, P. Balaguer, Evaluation of ligand selectivity using reporter cell lines stably expressing estrogen receptor alpha or beta, Biochem. Pharmacol. 71 (10) (2006) 1459–1469, doi:10.1016/j.bcp.2006.02.002.